The Computation of Induced Drag with Nonplanar and Deformed Wakes

Ilan Kroo*
Stanford University
Stanford, California 94305

and Stephen Smith †
NASA Ames Research Center
Moffett Field, CA

Abstract

The classical calculation of inviscid drag, based on far-field flow properties, is re-examined with particular attention to the nonlinear effects of wake roll-up. Based on a detailed look at nonlinear, inviscid flow theory, the paper concludes that many of the classical, linear results are more general than might have been expected. Departures from the linear theory are identified and design implications are discussed. Results include the following: Wake deformation has little effect on the induced drag of a single element wing, but introduces first order corrections to the induced drag of a multi-element lifting system. Far-field Trefftz-plane analysis may be used to estimate the induced drag of lifting systems, even when wake roll-up is considered, but numerical difficulties arise. The implications of several other approximations made in lifting line theory are evaluated by comparison with more refined analyses.

Nomenclature

b	wing span
C_l	section lift coefficient
D	drag
$\vec{F}$	inviscid force
l	section lift
S	area
$\hat{n}$	unit normal vector
u, v, w	perturbation velocity components
U, V, W	velocity components
U_∞	freestream velocity
$\vec{V}$	local flow velocity
y	spanwise coordinate
ϵ	wake deflection angle
ϕ	velocity potential
Γ	circulation, vortex strength
ρ	fluid density

Subscripts

i	induced component
n	normal component
w	wake

Introduction

The classical analysis of induced (vortex) drag involves several simplifying assumptions, which although not strictly valid, lead to very simple and useful results. Numerous experiments have demonstrated that classical theory is sufficiently accurate to be used in many design applications, but quantitative estimates of the error introduced by some of the theory's approximations have not been established. Recent studies have suggested that these approximations may account for errors in induced drag calculations of five to ten percent.[1] Although a calculation of this small force to within five percent might be considered quite acceptable for some applications, such errors would have significant implications for wing design.

Recently, much attention has been focussed on the significance of wake shape on the computation of induced drag.[1-4] It has been suggested that the nonplanar geometry of the vortex wake caused by self-induced roll-up or produced as a result of wing planform shape leads to a significant reduction in induced drag.[5,6]

In this paper, the classical calculation of inviscid drag, based on far-field flow properties, is re-examined with particular attention to the nonlinear effects of wake shape.

A Generalized Look at Classical Theory

The classical expression for the induced drag of a planar wing was derived by Prandtl, based on his lifting line theory[7]:

$$D_i = \int_{span} \frac{w}{U_\infty} l(y) dy \qquad (1)$$

* Assistant Professor, Department of Aeronautics and Astronautics
† Aerospace Engineer, Advanced Aerodynamic Concepts Branch

However, the lifting line assumption is more restrictive than necessary for this derivation. Munk[8] modeled lifting surfaces with sweep and systems of nonplanar elements with horseshoe vortices and showed that the drag could be written in terms of the far-field induced velocities:

$$D_i = \frac{\rho}{2} \int_{wake} \Gamma V_n \, dl \tag{2}$$

where V_n is the normal component of the induced velocity at the wake far downstream of the wing and Γ is the circulation on the wing at the corresponding spanwise position.

Reference 9, among others, shows how a similar result could be obtained without reliance on the simple vortex model. The drag may be related to the pressure and momentum flux over a control volume as shown in figure 1. In incompressible flow the force is given by:

$$\vec{F} = \frac{\rho}{2} \iint_S \vec{V}^2 \hat{n} \, dS - \rho \iint_S \vec{V}(\vec{V} \cdot \hat{n}) \, dS \tag{3}$$

so the drag is:

$$D_i = \frac{\rho}{2} \iint_{a,f} (\vec{V}^2 - 2U^2) \, dS - \rho \iint_{l,r,t,b} U(\vec{V} \cdot \hat{n}) dS \tag{4}$$

Equation 4 is based solely on the momentum equation for steady ideal fluid flow.

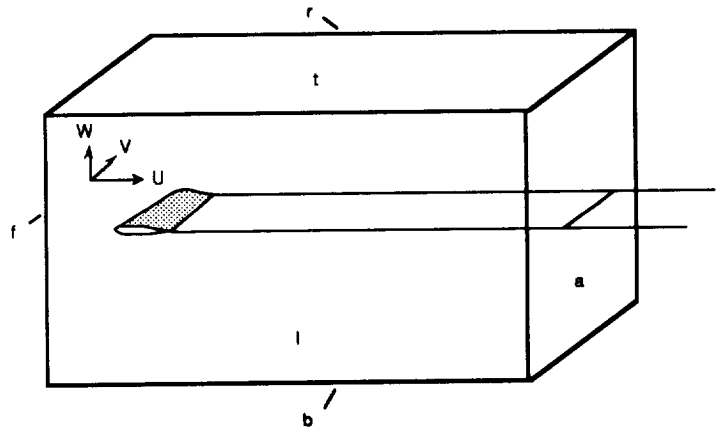

Figure 1. Control Volume for Computation of Forces.

This expression for drag may be written in terms of the perturbation velocities, u, v, and w:

$$D_i = \frac{\rho}{2} \iint_{a,f} v^2 + w^2 - u^2 - 2uU_\infty$$

$$-\rho \iint_{t,b} Uw - \rho \iint_{r,l} Uv \tag{5}$$

where the notation a, f denotes that the integral over the forward face is subtracted from the value over the aft face.

Mass conservation requires that:

$$\rho \iint_{a,f} u - \rho \iint_{t,b} w - \rho \iint_{r,l} v = 0 \tag{6}$$

leaving only the following terms:

$$D_i = \frac{\rho}{2} \iint_{a,f} v^2 + w^2 - u^2$$

$$-\rho \iint_{t,b} uw - \rho \iint_{r,l} uv \tag{7}$$

As the control volume size is increased, the high order terms associated with the top, bottom, front, and sides of the box become small and one is left with:

$$D_i = \frac{\rho}{2} \iint_a v^2 + w^2 - u^2 \tag{8}$$

In the case of potential flow, the integral may be written as:

$$D_i = \frac{\rho}{2} \iint_a \left(\frac{\partial \phi}{\partial x}^2 + \frac{\partial \phi}{\partial y}^2 + \frac{\partial \phi}{\partial z}^2 - 2u^2\right) dS$$

$$= \frac{\rho}{2} \iint_a (\nabla \phi \cdot \nabla \phi - 2u^2) \, dS \tag{9}$$

Substituting the vector relation:

$$\nabla \phi \cdot \nabla \phi = \nabla \cdot (\phi \nabla \phi) - \phi \nabla^2 \phi$$

and noting that outside the wake, $\nabla^2 \phi = 0$, the drag equation becomes:

$$D_i = \frac{\rho}{2} \iint_a \nabla \cdot (\phi \nabla \phi) - 2u^2 \, dS \tag{10}$$

Separating the divergence into terms in the cross flow and the x-derivatives leaves:

$$D_i = \frac{\rho}{2} \iint_a \nabla_{yz} \cdot (\phi \nabla_{yz} \phi) \, dS + \frac{\rho}{2} \iint_a \frac{\partial}{\partial x} (\phi \frac{\partial \phi}{\partial x}) - 2u^2 \, dS \tag{11}$$

Gauss' theorem allows us to express the area integral in terms of a contour integral surrounding the wake discontinuities. In general:

$$\iint_S \nabla \cdot F dS = \oint_c F \cdot \hat{n} dl$$

so,

$$D_i = \frac{\rho}{2} \oint_c (\phi \nabla \phi) \cdot \hat{n}\, dl + \frac{\rho}{2} \iint_a \phi \frac{\partial u}{\partial x} - u^2\, dS \qquad (12)$$

since the component of $\nabla\phi$ in the normal direction is just $\frac{\partial \phi}{\partial n}$, the closed contour integral around the wake becomes a line integral on the wake:

$$D_i = \frac{\rho}{2} \int_{wake} (\Delta\phi \frac{\partial \phi}{\partial n})\, dl + \frac{\rho}{2} \iint_a \phi \frac{\partial u}{\partial x} - u^2\, dS \qquad (13)$$

The jump in potential at a given point in the wake is just the integral of $V \cdot ds$ from a point above the wake to a point below. Since the normal velocity is continuous across the wake, the integral is equal to the circulation on the wing at the point where this part of the wake left the trailing edge. Also, the normal derivative of ϕ is just the normal velocity. So, we recover equation 2 with the correction due to the deformed wake:

$$D_i = \frac{\rho}{2} \int_{wake} \Gamma V_n\, dl + \frac{\rho}{2} \iint_a \phi \frac{\partial u}{\partial x} - u^2\, dS \qquad (14)$$

When the wake is assumed to trail from the wing trailing edge in the direction of the freestream, no u perturbations due to the wake are produced and so, far downstream of the wing, the correction terms vanish. If one further assumes that the section lift is linearly related to the freestream velocity and the circulation Γ, equation 14 may be reduced to equation 1.

The vanishing of the correction term in equation 14 does not require that the wing be modeled as a lifting line, nor that the wake be planar, only that the wake trails from the lifting surface in straight lines parallel to the freestream. Sears[3] has suggested that when the wake is flat, but is displaced from the freestream direction, only small differences from the classical results are to be expected. However, even slow deformations of the wake can lead to large differences in induced drag as calculated from the Trefftz-plane integration. A simple demonstration of this is shown in figure 2. This hypothetical wake shape, which folds over on itself, leads to no perturbation velocities in the Trefftz plane as the vorticity on the left and right sides of the wing are forced to cancel. This is entirely non-physical – but so is the straight wake generally used in Trefftz-plane calculations. It is therefore not apparent that the usual induced drag analysis can be used to accurately compute induced drag, since the actual wake shape far downstream of the lifting surface is significantly deformed under the influence of its own velocity field.

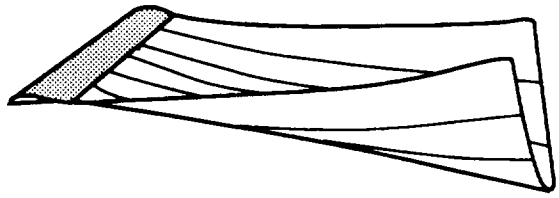

Figure 2. Hypothetical Wake Shape with Incorrect Far-Field Drag

This simple example illustrates that one must be very careful in applying Trefftz-plane analysis for induced drag prediction. In fact, even the general equation 4 will produce an incorrect result when applied in this case. The conditions under which it is acceptable to apply far-field analysis are easily determined by considering the two control volumes shown in figure 3. The force predicted from consideration of near-field velocities is:

$$\vec{F} = \oint_{NF} (...)\, dS = \oint_{FF} (...)\, dS - \oint_{wake} (...)\, dS$$

The far field analysis gives the correct result only when

$$\oint_{wake} (...)\, dS = 0$$

that is, when the wake is force-free. This means that correct results will be obtained when the wake shape is properly computed, including the deformation associated with induced velocities. If we are concerned only with the computation of drag, however, the conditions are somewhat less restrictive. The correct drag is obtained by far field analysis when the wake is drag-free. In the simple example of figure 2, the wake was not drag-free and this accounted for the clearly incorrect result. Although the correct force-free wake is drag free, it is not the only drag-free shape. A wake that trails downstream from the wing in the freestream direction must also be drag-free (as any forces are perpendicular to the direction of the vorticity). We are left with the very useful result that two wake

shapes may be used for calculation of the drag using far-field methods: the correct, rolled-up shape and the straight wake that is assumed for the classical theory. It should be noted that wakes are commonly placed in a body-fixed (not freestream-fixed) direction in many panel programs. Such practice leads to incorrect calculations based on far-field velocities, especially when the wake is nonplanar.

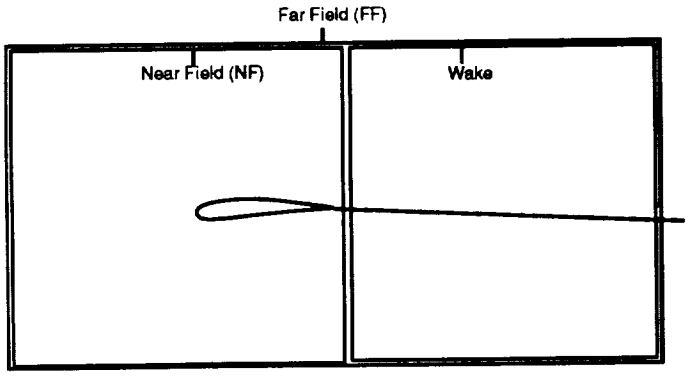

Figure 3. Control Volumes for Far-Field Drag Calculation

It is interesting to note that while the streamwise wake is acceptable for drag calculations, it is not, in general, valid for computation of lift in the far field. When lateral velocities (due to nonplanar geometries) act on a streamwise wake, lift forces are generated. This is why nonlinear lift effects are not seen as an increase in wake vorticity strength. Proper computation of these effects, including vortex lift, in the far field require consideration of wake deformation.

Influence of Wake Roll-Up on Drag

Although far-field computations are permissible when the wake is properly rolled-up or when the wake is in the direction of the freestream, the two results would not be expected to produce exactly the same result. One may argue, as Prandtl does in reference 7, that if the wake deforms slowly then the velocities produced by the deformed wake in the near-field should not be very different from the velocities produced by the straight wake in the near field. So a reasonable approximation may be obtained by assuming a straight wake and using the far-field integral on the simple wake shape. This is, in most practical cases, the best solution, but here we consider the approximation in more detail.

When the wake is assumed to be planar, but deflected by an angle, ϵ, from the freestream, the w^2 term in equation 8 is reduced by $\cos^2 \epsilon$ and the u^2 term is approximately $w^2 \sin^2 \epsilon$, leading to a change in drag of order ϵ^2. We note that for this planar wing, such a wake is drag-free and we expect the far-field solution to be valid. However, the correct wake shape is quite different from the simple deflected planar wake.

To provide a quantitative estimate of the effect of wake roll-up on drag, several wings were analyzed using the high order panel method, A502.[10] Drag was computed using surface pressure integration with a very refined panel geometry. The geometry of the wake network was computed using a separate vortex tracking method. The results for an aspect ratio 7 wing with an unswept trailing edge and an elliptical chord distribution show less than a 1% change in lift and less than 0.5% change in induced drag at fixed lift when the wake is rolled-up. Recent results of reference 11 illustrate similar behavior.

Part of the small difference in results produced with streamwise and rolled-up wakes is associated with the change in the lift distribution. In general, the shape of the lift distribution changes with angle of attack, since even the straight, freestream wake does not lie in the plane of the wing, and changes its orientation with respect to the wing as the freestream direction is varied. In the cases examined here, however, the trailing edge is straight and the lift distribution changes little with angle of attack, as shown in figure 4.

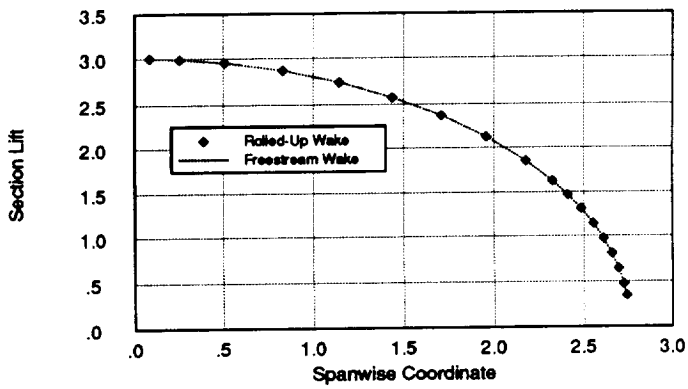

Figure 4. Effect of Wake Roll-Up on Lift Distribution

When the wing does not have a straight trailing edge, the situation is more complex. In such cases the near-field control volume that encloses the lifting surface is located so that some wake deformation has occurred before the

wake reaches the aft plane. Although the slow deformation of the wake downstream produces little effect on the velocities in this near-field plane, the initial deformation upstream of the plane can be important It is most significant when the wake is shed far forward of the near-field plane as in the case of staggered biplane systems. In this case, a substantial change in the effective vertical gap is possible.

Computational Approaches

Equation 8 may be used to compute the induced drag of a wing with a rolled-up vortex wake. However, it is inconvenient to evaluate this integral over a large area. Similarly, surface pressure integration requires extremely high panel densities to resolve the induced drag to within 1%. The simpler expressions that require velocities only over the intersection of the wake sheet with the Trefftz plane were based on the assumption of streamwise wake vorticity. The reduction of the 2-D integral to a line integral is not possible without approximation because of the presence of terms containing the perturbation velocity, u. Moreover, even when one ignores these terms, the resulting integral for drag is very sensitive to the computed wake shape. Figure 5 illustrates this conclusion. The induced drag was computed by rolling-up the wake behind an aspect ratio 7 wing with an unswept trailing edge and evaluating the normalwash far downstream. The induced drag values given by equation 2 resulted in a span efficiency factor of 1.035. Because of the sparse wake panel spacing in the area of y = 2.5, an additional panel was added as shown. Span efficiency was recomputed with the additional panel leading to a value of 1.082. Similar sensitivity was found to other changes in computed wake shape. Thus, not only is the computation of the wake shape time consuming, but the use of the usual 1-D drag integral is only approximate and the results are too sensitive to the roll-up calculation to be of practical value.

In summary, several approaches to the computation of induced drag with wake deformation are possible:

1) Evaluation of the Trefftz-plane wake integral (equation 2) is attractive since it involves 1-D integration; however, if wake deformation is considered the result is sensitive to the computed shape. In most cases, simple far-field calculations using a streamwise wake provide acceptable accuracy.

2) Surface pressure integration is a simple alternative, but requires extremely fine paneling to produce accurate results.

3) Evaluation of the perturbation velocities over the surface of a small control volume as in equation 7 is desirable when flow field information is available at these points. It should be noted that large canceling terms have been eliminated in equation 7 by consideration of mass conservation. This improves the accuracy of this method. The control volume should be large enough to avoid numerical errors associated with large gradients in the perturbation velocities, but small enough to produce acceptable computation times.

4) Equation 8 may be evaluated over a single "near-field plane". The area of integration must be expanded until convergence is achieved. Since the plane is placed near the trailing edge, results are less sensitive to errors in computed wake shape than are results of Trefftz-plane integration.

5) One may compute the initial roll-up of the wake sheet, extend the vorticity in the freestream direction, and evaluate the 1-D wake integral (equation 2) over the far wake. This provides an approximate result with most of the influence of wake deformation, little numerical error introduced from the wake shape calculation, and the simplicity of a one-dimensional integration.

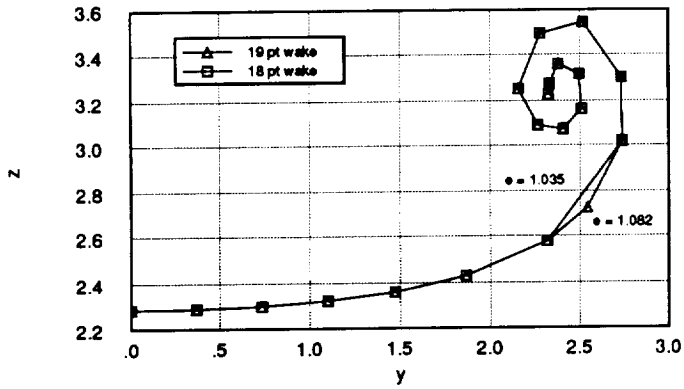

Figure 5. Effect of Computed Wake Shape on Span Efficiency from Far-Field Calculation

Additional Corrections

When one ignores the small differences between the freestream straight wake and the rolled-up wake there are still some differences between these results and those of lifting line theory. In many cases, these additional corrections, which are fully expected from the classical theory,

are more significant than the wake deformation considered previously.

Planform effects

Although the relatively large reductions in induced drag (8%) initially predicted for crescent-shaped wings has not been verified by subsequent, more refined analyses, smaller reductions (1-2%) in drag compared with the unswept elliptic wing planform have been shown. Such an improvement is not unexpected. Although the planar wake sheet due to an elliptic distribution of lift induces uniform downwash far downstream and at the start of the sheet, at other positions in the wake plane, the velocity perturbations are not uniform. Thus, while lifting line theory predicts an elliptic distribution of lift for an unswept, untwisted elliptic wing planform, lifting surface theory does not. A flat elliptical wing carries less lift near the tips than the elliptic load distribution. This can be corrected by sweeping the tips back, by increasing the chord near the tips, or by twisting the wing. The chord distribution of a wing with an unswept quarter chord line was modified until the lift distribution predicted by the A502 panel method was elliptic. The resulting planform shape is shown in figure 6 and results in an induced drag very similar to that of the crescent wing planform.

Figure 6. Wing Planform for Minimum Induced Drag with Fixed Span

Trailing edge shape and nonplanar wakes

Even if one assumes that the wake trails downstream in the freestream direction, modifications to the simplified theory are introduced by changes in wake shape. When the trailing edge of the wing is not straight, the wake appears nonplanar when viewed in the freestream direction (Figure 7). This means that its intersection with the Trefftz plane does not form a straight line. This, in turn, implies that the optimal span loading differs from the simple planar wing case and that the maximum span efficiency is greater than 1.0. This effect has been known for some time, mentioned first in connection with NACA tests of circular planform wings in the 1930's.[12] At more usual aspect ratios the effect is small, but in some cases measurable.

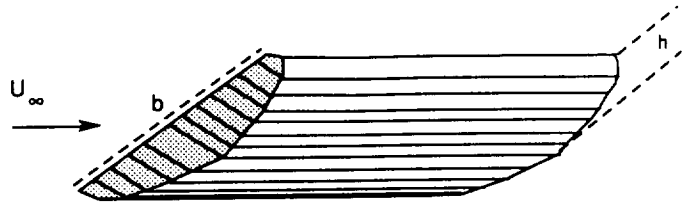

Figure 7. Curved Trailing Edges Lead to Nonplanar Wakes

Hoerner[13] also noted this effect in 1953, commenting that for wings with sweep, "the tips drop below the center part as the angle of attack is increased to positive values. The wing assumes in this way an inverted 'V' shape." Although Hoerner argues that this must increase induced drag, the nonplanar character of the wing viewed from the freestream direction may be used to reduce the induced drag below the minimum value for a planar wing. This idea has been further investigated by Burkett[5], and Lowson[6] who have computed minimum induced drag solutions for wings with nonplanar distributions of circulation when viewed in the freestream direction (Figure 8). Burkett views the wing as a swept lifting line along the quarter chord line and considers the resulting nonplanar projection in the freestream direction. Munk's stagger theorem suggests that the minimum drag of this configuration is equal to that of the unswept, nonplanar circulation distribution. Lowson expands on this idea, but notes that, "There are formal difficulties with this concept of camber-planform equivalence since lifting line theory and the Munk optimization are based on linearized Trefftz-plane analysis of the shed wake. The relation of the shed wake shape to the wing planform distribution remains unclear; for example, the actual wake shape at the trailing edge of the wing is not the same as the quarter-chord condition normally assumed." Although Munk did use such a lifting line concept in his derivation of the stagger theorem, it is completely unnecessary. The more general derivation of the expression for induced drag given in the preceding section does not make use of the lifting line concept at all. The induced drag depends only on the wake shape and the distribution of vorticity in the wake. Munk's stagger theorem, that the induced drag of a general distribution of circulation does not depend on the longitudinal position of the vortex elements, follows immediately. Munk's results, while originally derived based on the lifting line model, are much more general. (Munk later realized this and remarked that, "My principal paper on the induced drag was still under the spell of Prandtl's vortex theory...it was not the right approach.")

The derivation of the expressions for induced drag given here shows that drag is related only to the circulation distribution and the shape of the projected wake downstream. Thus, it is not the shape of the lifting line that is important, but rather the shape of the wake. Using the drag-free, streamwise wake and ignoring the effects of self-induced deformation, it is the shape of the wing trailing edge that determines the wake shape downstream. This suggests that wings with aft-swept tips and straight trailing edges should have no advantage from nonplanar wake effects, while wings with unswept leading edges would achieve a small savings. The 2% drag reduction at a lift coefficient of about 0.5 predicted by Burkett for a "crescent wing" with extreme tip sweep would be expected to be less than 1/3 this large when the trailing edge (rather than quarter-chord) curvature is used. A wing with an unswept leading edge, with the chord distribution or twist needed for optimal loading, should achieve a slightly greater savings. For wings with reasonable taper ratios in cruise, the potential for drag reduction is quite small; however, at higher angles of attack when trailing edge curvature is concentrated near the tip regions, more significant savings appear. When wake deformation occurs upstream of the most aft part of the trailing edge, the trace of the wake in the "near-field plane" defines the shape of the projected wake.

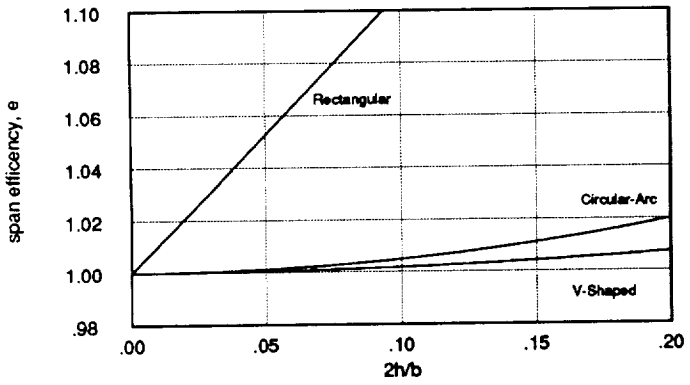

Figure 8. Effect of Nonplanar Streamwise Wakes on Minimum Induced Drag

Nonlinear lift

The relationship between vorticity in the wake and lift on the wing section is also more complex than indicated by the linear assumption of the simple classical theory. Figure 9 illustrates the distribution of lift, computed by surface pressure integration on an aspect ratio 7 wing with a straight trailing edge and elliptical chord distribution. The figure also shows the distribution of circulation, as reflected by the doublet strength in the streamwise wake. The computations were performed using the high order panel program, A502. Note that although the two curves match quite closely over much of the wing, a discrepancy appears in the tip region where the lift is larger than would be expected on the basis of liner theory. This nonlinear lift increment is associated with lateral induced velocities from the wake, increasing the local velocity $\vec{V}$ in the expression: $\vec{l} = \rho \vec{V} \times \vec{\Gamma}$ above the freestream value. These lateral velocities give rise to a lift increment through their interaction with the streamwise component of vorticity on the wing. This form of 'vortex lift' increases the overall lift, but does not change the magnitude of the shed vorticity. The total lift is increased, compared with the classical linear result, while the induced drag is unchanged (since the vorticity distribution in the wake is fixed), leading to higher span efficiency.

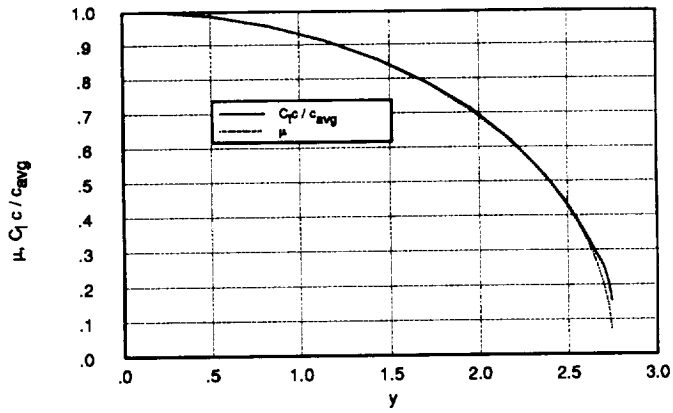

Figure 9. Distribution of Lift and Doublet Strength over a Planar Wing

Design Implications

It is of interest to examine the possibility of exploiting the differences between the more general results discussed here and those of lifting line theory. Although each of the effects is small, the combination of the following considerations might be used to produce a measurable drag reduction.

1) Wake deflection and roll-up leads to induced drag values slightly different from those computed using a streamwise wake; one might employ configurations that

take advantage of this effect. For single wings the effect is negligible, but for multiple lifting surfaces it is not. The effective vertical gap between two surfaces may be increased when the forward surface lies below or in the plane of the second surface. In this case, wake deflection has a first order effect on drag and is seen to be significant in the analysis of configurations such as joined wings, canard aircraft, and sailing vessels with twin keels or keel-rudder interference. In such cases, approximate results are best obtained by computing the wake deformation to a point downstream of the most aft surface, and then extending the wake streamwise beyond that point.

2) Lifting surface theory leads to the conclusion that an elliptic distribution of lift requires a non-elliptic chord distribution, or the inclusion of sweep or twist. Straight, untwisted elliptical wings achieve a lift distribution that has 1-2% more drag than the theoretical minimum associated with an elliptical circulation distribution.

3) The wake of an inclined planar wing with a curved trailing edge forms a nonplanar sheet, even when the wake vorticity is projected in the streamwise direction. This effect increases with angle of attack and is most important for low aspect ratio wings. An aspect ratio 7 elliptic wing with straight leading edges and an optimal distribution of lift would be expected to save 1-2% in cruise induced drag compared with a wing with a straight trailing edge. Larger tip chords and higher angles of attack provide the potential for greater savings.

4) Exploiting the nonlinear lift increments associated with lateral induced velocities further increases span efficiency. This leads to somewhat larger tip chords than would be expected from linear theory. The extra lift leads to induced drag values at fixed lift of order 0.5% lower than predicted by linear theory.

Of course, the design of wings involves considerations such as high-lift performance, structural weight, fuel volume, and buffet, making it impossible to relate the above effects to changes in optimal planform shape without refined multidisciplinary analysis. The same is true of the design of bird's wings and fish tails and it seems unlikely that the effects mentioned here are responsible for the oft-cited aft-swept wing-tips and fins of these animals. The small effects on induced drag are likely overshadowed by the requirements associated with folding wings, or shedding seaweed.

Conclusions

The basic results of the classical aerodynamic theory of induced drag, derived without reliance on the simple lifting line model, demonstrate the approximations involved in the usual simple formulas for vortex drag. Numerical analysis of simplified vortex systems and of more refined wing models illustrate the following conclusions:

Trefftz-plane calculations are appropriate for rolled-up wakes or freestream wakes. The latter is a more practical approach given sensitivities to the computed shape.

Perhaps more important than wake roll-up are several additional approximations made by the simplest of classical analyses, lifting-line theory. Such analysis generally does not include effects such as the nonuniform downwash of an elliptically-loaded wing near its origin, the nonplanar character of the wake shed from a curved trailing edge, and the nonlinear relationship between section lift and circulation especially in the region of wing tips.

Although none of these effects is large for typical high aspect ratio wings at moderate angles of attack, the combined effect is important in the accurate evaluation of induced drag.

Acknowledgement

This research was supported by a Grant from NASA Ames Research Center, NCC2-683.

References

1. Van Dam, C. P., "Induced Drag Characteristics of Crescent-Moon-Shaped Wings," Journal of Aircraft, Vol. 24, No. 2, 1987, pp. 115-119.

2. van der Vooren, J., Sloof, J.W., "CFD-Based Drag Prediction: State of the Art, Theory, Prospects," NLR Technical Publication TP 90247 L, August 1990.

3. Sears, W.R., "On Calculation of Induced Drag and Conditions Downstream of a Lifting Wing," *Journal of Aircraft*, Vol. 8, March 1974, pp 191-192.

4. McCuthchen, C.W., " Induced Drag and the Ideal Wake of a Lifting Wing," *Journal of Aircraft*,Vol. 26, No. 5, May 1989, pp 489-493.

5. Burkett, C.W., "Reductions in Induced Drag By the Use of Aft-Swept Wing Tips," *Aeronautical Journal*, Vol. 93, December 1989, pp 400-405.

6. Lowson, M.V., "Minimum Induced Drag for Wings

with Spanwise Camber," *Journal of Aircraft*,Vol. 27, No. 7, July 1990 pp 627-631.

7. Prandtl, L., "Applications of Modern Hydrodynamics to Aeronautics", NACA Rept. 116

8. Munk, M., "The Minimum Induced Drag of Aerofoils," NACA Rept. 121, 1921.

9. Landau, L., Lifshitz, E., *Fluid Mechanics*, Pergammon Press, 1959.

10. Smith, S.C., Kroo, I., "A Closer Look At the Induced Drag Characteristics of Crescent-Shaped Wings," AIAA Paper No. 90-3063, August 1990.

11. DeHaan, M., "Induced Drag of Wings with Highly-Swept and Tapered Wing Tips," AIAA PAper No. 90-3062, August 1990.

12. Zimmerman, C.H., "Characteristics of Clark-Y Airfoils of Small Aspect Ratios," NACA Rept. 431, 1932.

13. Hoerner, S.F., *Fluid Dynamic Drag*, Hoerner, 1953.